Robotica (2014) volume 32, pp. 1301–1316. © Cambridge University Press 2014
doi:10.1017/S0263574714001519

Human-adaptive control of series elastic actuators

Andrea Calanca* and Paolo Fiorini

Department of Computer Science, University of Verona, Verona, Italy

(Accepted May 19, 2014. First published online: July 7, 2014)

SUMMARY

Force-controlled series elastic actuators (SEAs) are the widely used components of novel physical human–robot interaction applications such as assistive and rehabilitation robotics. These systems are characterized by the presence of the "human in the loop" so that control response and stability depend on uncertain human dynamics. A common approach to guarantee stability is to use a passivity-based controller. Unfortunately, existing passivity-based controllers for SEAs do not define the performance of the force/torque loop. We propose a method to obtain predictable force/torque dynamics based on adaptive control and oversimplified human models. We propose a class of stable human-adaptive algorithms and experimentally show advantages of the proposed approach.

KEYWORDS: Force control; Series elastic actuators; Soft/compliant actuators; Rehabilitation robotics; Physical human–robot interaction; Adaptive control; Exoskeletons, Haptic interfaces.

1. Introduction

Most of the modern rehabilitation robotic systems make use of force-controlled joints following the "assist as needed" paradigm. In this approach, the patient is delicately guided to a target trajectory, progressively reducing the interaction forces as the patient learns to better follow a desired path. In fact, it has been shown that patients should be active to enable the motor learning process,[3,9,12] thus rehabilitative devices should not be coercive. Several control algorithms have been proposed following this "assist as needed" approach, e.g. "path control," "virtual model control," "clime," gravity compensation,[6,13] or impedance control.[25] This class of algorithms is built upon a force/torque controller that is supposed to be ideally fast. However, when the algorithm is implemented, the force variable cannot be commanded instantaneously and its transients depend on both robot and patient dynamics. In particular, using a traditional controller we can have slow force/torque responses when the patient displays a low mechanical impedance, and force/torque overshoots when the patient has a high impedance configuration. These effects are undesirable because they can generate disturbances that interfere with rehabilitation strategy and even potentially lead to instability and patient injuries.

Currently, a widely used method to guarantee stable human–robot interaction is based on passivity-based (PB) control. Despite the complexity of passivity formalism, PB control is quite straightforward to implement[16,24] and the whole stability can be guaranteed by assuming that humans behave in a passive way. Unfortunately, in PB control it is not possible to give any servo specification because the controller needs to be stable against any kind of external passive environment, no matter what kind of environment and its scale, i.e. its level of inertia, stiffness, or damping. It follows that this approach is very conservative, and by completely neglecting environmental dynamics, it is not possible to speculate on control performance. It must be said that this limit is not due to passivity itself but due to the absence of a human model. As a matter of facts, authors proposing passive controllers for rehabilitation or physical human–robot interaction (pHRI) usually do not comment on control tuning (that involves specifications). The implicit idea is of tuning the system by trial and error, considering an average human dynamics and trying to match a desired transient. Then it is necessary to check if passivity constraints are satisfied.[24] However, this strategy leads to the following considerations:

* Corresponding author. E-mail: andrea.calanca@gmail.com

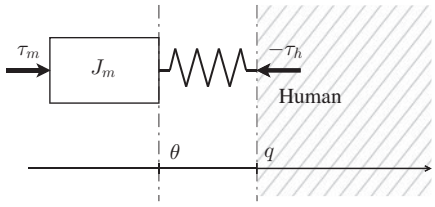

Fig. 1. Model for series elastic actuator proposed in ref. [16]. It includes the motor inertia, the elasticity, and the coupling with the environment.

1. In our experience,[5] it is quite difficult to carry out a tuning process with the human in the loop from the point of view of both safety and practical feasibility. Of course, it is possible to couple the system to an artificial limb or a manikin, but in these cases the solution will be quite approximate.
2. The tuning session can be time-consuming. In fact, if the passivity conditions are not satisfied in the first trial, it is necessary to reiterate tuning until passivity is finally archived. In fact, there is no method to verify passivity during the tuning process unless a very simple control structure is assumed.
3. Pathologies can specifically affect limbs. With currently available PB controllers, the tuning procedure should be carried out separately for each patient and patient joint. It follows that an automatic tuning process can be of paramount importance.
4. Humans typically change their dynamics in response to the environment and depending on specific tasks. For example, leg dynamics dramatically changes between the swing and the stance phase. Also, damping and stiffness can be increased by muscle co-contraction, e.g. when we want to make a precise positioning, or when we hold heavy loads.

To solve these issues, we propose a model-based controller that automatically varies force control gains in response to changing conditions to match the desired force/torque transient. Since the whole human modeling is too complex, it is reasonable to think that a simplified model can tell us at least something about the patient. In particular, we approximate human joints and endpoints with second-order linear models. Combining such a generic models with adaptivity, we meet two objectives: First, using a generic model we can account for a generic human joint, and second, using adaptivity we can update model parameters as the situation changes, e.g. when a grasped mass is added or when co-contraction is modified. We propose an approach inspired by model reference adaptive control (MRAC) where control specifications can be determined by the reference model, letting the tuning process be automatic and online adapting to changing conditions.

The paper is organized as follows. Section 2 presents the currently available solutions for series elastic actuator (SEA) control in pHRI. Section 3 describes the system to be controlled, and Section 4 introduces the proposed adaptive controller and gives a theoretical stability analysis. Experimental results are presented in Section 5. Finally, conclusions are drawn in Section 6 together with the future work plan.

2. Series Elastic Actuators and Their Control

2.1. Series elastic actuators and force control

Series elastic actuators have been proposed to overcome force control difficulties that arise using stiff actuators.[16] In SEAs a spring is arranged between the motor and the environment, which in our case is a generic human joint. This is shown in Figure 1, where τ_m is the motor force/torque, k is the series spring stiffness, θ is the motor position, τ_h is the human interaction force/torque, and q is the human joint position. The relation among these variables can be expressed as

$$\tau_h = k(\theta - q), \tag{1}$$

$$J_m\ddot{\theta} = \tau_m - \tau_h, \tag{2}$$

where the first equation describes the force exerted by the spring on the human, and the second accounts for motor inertia, J_m.

https://doi.org/10.1017/S0263574714001519 Published online by Cambridge University Press

The main advantages of SEAs are the increased force control robustness, augmented shock tolerance, and safety due to lower reflected inertia. Moreover, force can be measured through spring deformation that is cheaper than using a load cell (in the case of force) or a rotative torsiometer (in the case of torque).

To the authors' knowledge, all proposed SEA implementations make use of high transmission ratios. For example: In ref. [17] a ball screw with a pitch of 2 mm per revolution (linear actuator) is used, whereas in ref. [11] the transmission ratio is $n = 130$ (rotative actuator). The reason why SEAs usually employ reducers or gearboxes is to obtain high force and high power density. However, a geared motor is very stiff and difficult to control in force. By adding a series spring, SEAs transform the force control problem into a position control problem (spring displacement) where high ratio transmissions are known to be helpful: the motor results stiffened and the effects of external disturbances are reduced.

2.2. Series elastic actuators and robust interaction control

Currently the main technique used to stabilize pHRI is based on the passivity theory. PB controllers are quite easy to implement and impressively robust as they are stable when coupled to *any* passive environment. However, nothing can assure us that a PB controller is a "good controller." For example, the PB force controller proposed in ref. [16] consists of a standard proportional-integral-derivative (PID) controller with an integral roll-off, as represented by

$$F(s) = P + \frac{Ds}{1 + T_d s} + \frac{I}{1/T_i + s}, \tag{3}$$

where P, D, and I are positive gains and the integral roll-off must satisfy $T_i \leq \sqrt{D/I}$. The performance of this passive PID controller depends on both gain values and coupled environment whose dynamics is usually unknown and produces unknown control performance. For passivity analysis of different control architectures, including inner velocity loops and pure integrators, the reader can refer to ref. [24], where it is shown that, depending on the architecture, the passivity constraint imposes upper or lower bounds on certain control gains. About passivity, Hogan[1] reported that "discrete control, time delays, actuator and sensor limitations, and unmodeled dynamics can also compromise passivity, making the implementation of passive control on real systems extraordinarily challenging."

A significantly different approach to pHRI control is described in ref. [23] and is based on classic robust control and not on elastic actuators. This method potentially allows to account for specifications, but it needs an accurate human model which is very hard to develop in practice. Another robust strategy has been applied to the case of a stiff motor and is reported in refs. [1, 2]. Here the authors consider oversimplified models (linear second-order) for the human, and propose an automated procedure to search for a robust controller which is optimal in terms of both performance and stability. This is because most of classic robust methods provide only analysis tools to check the stability at the end of a design phase, and in case of failure it is necessary to iterate between the design and the analysis phases. Also, the robust design is a sub-optimal solution because the assumed model set needs to be conservative to include uncertainties.

3. System Analysis

In this work, we follow the approach of using second-order linear models to approximate the human joint impedance.[1] Such a simple and general models have two main advantages. First, they need fewer parameters to be adapted to. Second, a single adaptive controller structure can work for every human joint and also for human endpoints, broadening the applicability of the approach.

In the first step, we model the system by considering the human joint as a pure inertia, J_h. In this case we have the following human model

$$J_h \ddot{q} = k(\theta - q) = \tau_h \tag{4}$$

[1] Although this oversimplification is quite rough, it is widely used (and tested) in the literature, see, for example refs. [10, 15, 20–22, 26].

https://doi.org/10.1017/S0263574714001519 Published online by Cambridge University Press

to be considered together with SEA models (1) and (2). To describe the torque control application, the overall model should be arranged with an input torque τ and an output torque τ_h. To this aim, it is possible to rewrite (1), (2), and (4) as

$$\frac{J_m}{k}\ddot{\tau}_h + \left(1 + \frac{J_m}{J_h}\right)\tau_h = \tau. \tag{5}$$

Note that this torque to torque relation gives a second-order system in spite of being originally a fourth-order system. The reason is that if we do not account for friction and/or human joint stiffness, we have pole-zero cancellations. Thus, the second-order approximation is reasonable only in the case of a pure inertial load, otherwise a higher order system should be considered. In particular, the model becomes the third-order in the presence of human joint damping, and the fourth-order if we account also for stiffness, leading to the following equations:

$$\frac{J}{k}\ddot{\tau}_h + \left(1 + \frac{J_m}{J_h}\right)\tau_h - rh(q - q_0) - rd\dot{q} = \tau, \tag{6}$$

$$J_h\ddot{q} = \tau_h - h(q - q_0) - d\dot{q}, \tag{7}$$

where $r = \frac{J_m}{J_h}$. The structure of human joint model (7) can be used to represent both passive and active human conditions. In the passive human condition the stiffness term $h(q - q_0)$ can be considered as a linear approximation of gravitational torque, and the damping term $d\dot{q}$ describes the mechanical joint friction due to muscle, tendons, and articulations. In the active human condition the human is supposed to actively control the joint to reach the position q_0, and the damping and stiffness terms are mainly due to muscle contraction/co-contraction.

In both models (5) and (6), the dynamics of τ_h depends on two parameters:

$$a = \frac{J_m}{k},\ c = (1 + \frac{J_m}{J_h}) = 1 + r. \tag{8}$$

Interestingly, the inertia uncertainty is lumped in c, while a can be known *a priori*, as it characterizes the actuator. In the control application, the worst case is when c, or equivalently r, is high, showing high sensitivity to the human joint model. This can be seen in (6) where r multiplies human forces/tuques. Unfortunately, this is often the case of SEAs where geared motors are usually adopted. In fact, the (reflected) motor inertia J_m, which is proportional to r, acts as a sensitivity gain. If one considers that the reflected motor inertia is augmented by a factor n^2, where n is the transmission ratio, it follows that in most applications the system can be very sensitive to uncertainties.

4. System Control

In the MRAC framework, control specifications are given using a model reference. This is particularly convenient when it is easy to specify the desired bandwidth and damping/overshoot as in the linear second-order reference model. However, in MRAC the reference model should have the same order as the plant to ensure adaptation convergence (perfect tracking assumption). In this work, we propose a slightly modified approach to use the second-order reference model even if the system (6)–(7) is of fourth order.

Let's start by considering the following model reference:

$$\ddot{\tau}_r(t) + \lambda_1\dot{\tau}_r(t) + \lambda_2\tau_r(t) = \lambda_2 r(t), \tag{9}$$

where parameters λ_1 and λ_2 are chosen according to the desired bandwidth and damping of the controlled system, and $\tau_r(t)$ is the desired torque dynamics for τ_h in response to the bounded reference input $r(t)$.

If we consider the pure inertial model (5), we can achieve perfect tracking using the following control law:

$$\tau_m = a(\ddot{\tau}_r - 2\lambda\dot{e} - \lambda^2 e) + c\tau_h, \tag{10}$$

https://doi.org/10.1017/S0263574714001519 Published online by Cambridge University Press

where $e = \tau_h - \tau_r$ is the error between the system torque and the reference model torque, λ is the positive design parameter, and a, c are defined in (8). If we compute the closed loop dynamics, we obtain exponential convergence to the reference model with rate λ, that is

$$\dot{s} + \lambda s = 0, \tag{11}$$

where $s = \dot{e} + \lambda e$ is the measure of the tracking error whose convergence ($s \to 0$) implies the convergence of e and $\dot{e}$ ($e \to 0$, $\dot{e} \to 0$) (see ref. [19, Section 7.1.1]).

Inertia uncertainty can be taken into account by substituting the parameter c in (10) with its estimate $\hat{c}$, provided that

$$\dot{\hat{c}} = -\gamma s \tau_h, \tag{12}$$

where γ is the adaptation gain to control the estimation speed. Stability of this adaptive controller can be proven within the standard MRAC framework, as reported in the Appendix. Unfortunately, this stability analysis is not valid when considering the fourth-order system (6)–(7) as discussed earlier. This invalidates the perfect tracking assumption and the stability analysis in the Appendix. To overcome this problem, we propose some candidate controllers that retain the simplicity of the second-order reference model, but are stable when applied to the system (6)–(7), which is of higher order. The standard MRAC approach would lead to a more complex control structure (to reach perfect tracking) and higher dimensional estimation. Also, we would lost the smart parametrization of models (5) and (6) where (known) actuator parameters are separated from (unknown) human parameters, i.e. coefficient a does not depend on human dynamics. In the following we propose first a controller based on five parameter estimates, then we show that the number of estimates can be reduced while increasing stability robustness.

4.1. An adaptive controller for SEAs

The first controller that we propose is based on the compensation of certain dynamics aiming to make the τ/τ_h relation behaving like a second-order system. We consider an arranged version of system (6),

$$a\ddot{\tau}_h + b\dot{\tau}_h + c\tau_h = \tau_m + h^*\theta - h_0 + d^*\dot{\theta}, \tag{13}$$

where, naming $r = \frac{J_m}{J_h}$, we have the following parameters: $a = \frac{J_m}{k}$, $b = r\frac{d}{k}$, $c = 1 + r(1 + \frac{h}{k})$, $h^* = rh$, $h_0 = h^* q_0$, and $d^* = rd$. Parameter a is known *a priori*, while the others depend on human dynamics. The advantage of adopting this arrangement is that with respect to (6) it explicitly shows the full dynamics of the interaction torques (all the τ_h derivatives) and contains only collocated variables. In fact, non-collocated feedback is known to have lower stability margins. In practical applications, where it is quite usual to have unmodeled dynamics, combining adaptivity with low gain margins can actually present a risk of instability. In light of this consideration, we propose the following adaptive controller:

$$\tau_m = a(\ddot{\tau}_r - 2\lambda\dot{e} - \lambda^2 e) + \hat{b}\dot{\tau}_h + \hat{c}\tau_h - \hat{h}\theta - \hat{d}\dot{\theta} + \hat{h}_0 - \delta, \tag{14}$$

$$\dot{\hat{b}} = -\rho s\dot{\tau}_h \quad \dot{\hat{c}} = -\rho s\tau_h \quad \dot{\hat{d}} = -\rho s\dot{\theta} \quad \dot{\hat{h}} = -\rho s\theta \quad \dot{\hat{h}}_0 = -\rho s, \tag{15}$$

where $s = \dot{e} + \lambda e$, $e = \tau_h - \tau_r$ is the error with respect to the reference model (9) and ρ is an adaptation gain. In the following theorem we prove that this control law can stabilize the fourth-order system (6)–(7) by using a second-order reference model. This result will be used also in the rest of the paper, and, in our opinion, it is an original contribution. To achieve the proof we introduce in the control law the term

$$\delta = \epsilon\frac{e}{s}\dot{q}, \tag{16}$$

where ϵ is an arbitrarily small positive parameter. Note that λ is usually chosen as high as possible, thus in practice $\delta \simeq \frac{\epsilon}{\lambda}\dot{q}$ approximates the form of a damper.

https://doi.org/10.1017/S0263574714001519 Published online by Cambridge University Press

THEOREM 1. *Given system (6)–(7) where τ is determined by the adaptive control law (14) with adaptation (15) and assuming a steady state reference model condition $\tau_r(t) = \bar{\tau}_r$, then the trajectories of states e, $\dot{e}$, $\dot{q}$ are asymptotically stable (AS) and estimation errors and q are marginally stable.*

Proof. Consider the following Lyapuanov function $V(t) = V_s(t) + V_q(t) + V_p(t)$, where

$$V_s(t) = \frac{1}{2}as^2, \;\; V_q(t) = \frac{1}{2}f\tilde{q}^2 + \frac{1}{2}g\dot{q}^2 \tag{17}$$

with $\tilde{q} = q - \bar{q}$, $\bar{q} = \frac{\bar{\tau}_r}{h} + q_0$, and

$$V_p(t) = \frac{1}{2\rho}(\tilde{b}^2 + \tilde{c}^2 + \tilde{d}^2 + \tilde{h}^2 + \tilde{h}_0^2), \tag{18}$$

where naming p a generic parameter, $\tilde{p}$ represents the parameter estimation error $\tilde{p} = \hat{p} - p$. For better understandability, we first prove the stability assuming perfect estimation. In such a case the closed loop dynamics is $a(\dot{s} + \lambda s) = -\delta$, and the Lyapuanov time derivative is

$$\dot{V}_s = as\dot{s} = -a\lambda s^2 - s\delta. \tag{19}$$

For states q and $\dot{q}$, we have $\dot{V}_q = fq\dot{q} - f\bar{q}\dot{q} + g\dot{q}\ddot{q}$, and from (7) we have $\dot{q}\ddot{q} = \frac{1}{J_h}[\tau_h\dot{q} - h(q\dot{q} - q_0\dot{q}) - d\dot{q}^2]$ and, by choosing $f = h\epsilon$ and $g = J_h\epsilon$, we find

$$\dot{V}_q = \epsilon(\tau_h\dot{q} + hq_0\dot{q} - h\bar{q}\dot{q} - d\dot{q}^2).$$

Now substituting δ as in (16) and considering that $\tau_h = e + \bar{\tau}_r$, we obtain $\dot{V} = -a\lambda s^2 + \epsilon\dot{q}(\bar{\tau}_r + hq_0 - h\bar{q}) - \epsilon d\dot{q}^2$. Finally, we eliminate the second term by substituting the expression of $\bar{q}$, leading to

$$\dot{V} = -a\lambda s^2 - \epsilon d\dot{q}^2 \leq 0. \tag{20}$$

If now we introduce the parameter dynamics, the estimation errors appear in

$$\dot{V}_s = -a\lambda s^2 + s(\tilde{b}\dot{\tau}_h + \tilde{c}\tau_h + \tilde{d}\dot{\theta} + \tilde{h}\theta + \tilde{h}_0) - s\delta. \tag{21}$$

Summing $\dot{V}_p = \frac{1}{2\rho}(\tilde{b}\dot{\tilde{b}} + \tilde{c}\dot{\tilde{c}} + \tilde{d}\dot{\tilde{d}} + \tilde{h}\dot{\tilde{h}} + \tilde{h}_0\dot{\tilde{h}}_0)$ and substituting the proposed adaptation (15), one obtains $\dot{V}_{s+p} = -a\lambda s^2 - s\delta$, which is equal to (19). Then the demonstration proceeds as in the previous case leading to (20) that implies global marginal stability for state trajectories. Finally, using Barbalat's lemma it can be proved that states s, $\dot{q}$ are asymptotically stable. □

4.2. A simpler and more robust adaptive controller

The control strategy proposed in the previous section is theoretically sound and we will show in Section 5 that under certain conditions it works with very high performance. However, it is known that such a multi-dimensional estimation can be a hazard in practice, especially when there is a mismatch between the model structure and the human dynamics and/or we do not have persistent excitation. We show that using fewer parameters it is possible to have performance similar to algorithm (14) with increased robustness, i.e. we can consider a more generic human joint model

$$J_h\ddot{q} + Z_h(q, \dot{q}, q_0) = \tau_h, \tag{22}$$

where Z_h represents nonlinear stiffness and damping forces. With respect to (7), this is a more realistic description because the human muscles are strongly nonlinear. As muscle forces are also limited, we introduce the following bound:

$$|Z_h(q, \dot{q}, q_0)| \leq \Omega \tag{23}$$

https://doi.org/10.1017/S0263574714001519 Published online by Cambridge University Press

with $\Omega \geq 0$. By using this joint model, the interaction dynamics can be rewritten as

$$a\ddot{\tau}_h + c\tau_h = \tau + rZ_h(q, \dot{q}, q_0) \tag{24}$$

with parameters a and c as defined in (8) and $r = \frac{J_m}{J_h}$. We propose the following control law:

$$\tau_m = a(\ddot{\tau}_r - 2\lambda\dot{e} - \lambda^2 e) + \hat{c}\tau_h \tag{25}$$

with adaptation

$$\dot{\hat{c}} = -\rho(s\tau_h + \sigma\hat{c}), \tag{26}$$

where $e = \tau_h - \tau_r$ is the error with respect to the reference model (9) and $s = \dot{e} + \lambda e$. Parameter ρ is an adaptation gain and σ is the forgetting factor that was introduced in ref. [14].

THEOREM 2. *Given system (24), with the assumption of bounded human forces (23), and the adaptive control law (25)–(26), then the state trajectories $s(t)$ and $\tilde{c}(t)$ are globally uniformly ultimately bounded (UUB).*

Proof. Consider system (24), where we have a known *a priori*. Consider the Lyapuanov function $V(t) = V_s(t) + V_p(t)$ with V_s as before in (17) and $V_p = \frac{1}{2\rho}\tilde{c}^2$. By applying the control law (25) with adaptation (26) to system (24), (23) we find

$$\begin{aligned} \dot{V}_s &= as\dot{s} = -a\lambda s^2 + srZ_h + s\tilde{c}\tau_h, \\ \dot{V}_p &= \tfrac{1}{\rho}\tilde{c}\dot{\tilde{c}} = -s\tilde{c}\tau_h - \sigma\tilde{c}^2 - \sigma c\tilde{c}, \end{aligned} \tag{27}$$

where $\tilde{c} = \hat{c} - c$. By summing $\dot{V}_s$ and $\dot{V}_p$, we have

$$\dot{V} = -a\lambda s^2 + rZ_h s - \sigma\tilde{c}^2 - \sigma c\tilde{c}. \tag{28}$$

Then, if we analyze the Lyapuanov derivative outside the region

$$-a\lambda s^2 + srZ_h - \sigma\tilde{c}^2 - \sigma c\tilde{c} = 0, \tag{29}$$

we have $\dot{V} < 0$. Thus, outside (29) the trajectory behaves as if the origin was uniformly asymptotically stable. Consequently, the function V will continue decreasing until the trajectory enters the region (29) in finite time and remains there. Formally by choosing β such that $|\beta| > r\Omega$, we have that $\dot{V} < 0$ is satisfied on every boundary expressed as

$$a\lambda s^2 - s\beta + \sigma\tilde{c}^2 + \sigma c\tilde{c} = 0, \tag{30}$$

meaning that trajectories $s(t)$ and $\tilde{c}(t)$ are globally uniformly bounded. Moreover, an ultimate bound can be computed by substituting $\beta = r\Omega$ in (30). □

It is easy to show that the boundary area decreases monotonically with λ, and that boundedness of s implies boundedness of $e(t)$ and $\dot{e}(t)$ (see for proof, ref. [19, Section 7.1.1]). We conclude that by a proper choice of λ the attracting region can be sufficiently small and we can have acceptable tracking errors. Figure 2 graphically represents the attracting region (30) in the state plane (left) and in the error phase plane (right).

Theorem 2 is again, in our opinion, original. In fact, with respect to standard MRAC, control law (25) embeds only a partial system model, as it discards the dynamics of q and $\dot{q}$.

An interesting observation is that a high human joint inertia helps to improve accuracy (this is because β decreases with J_h). In fact, the control task is usually facilitated in case of high coupled impedance. Here we explain this effect for model (6)–(7). If we consider the limit cases of infinite damping or stiffness ($h \to \infty$ or $d \to \infty$) then the human joint position q becomes infinitely stiff,

https://doi.org/10.1017/S0263574714001519 Published online by Cambridge University Press

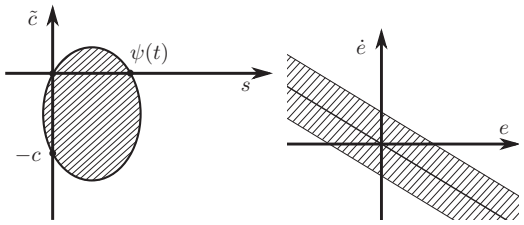

Fig. 2. On the left we draw a representation of the attracting region (29) where $\psi(t) = rZ_h$. When Z_h is negative, the region is mirrored on negative x-axis. On the right we represent only the states e, $\dot{e}$, and one can see the region mapped on the error phase plane.

thus imperturbable. This makes the system model (6)–(7) become

$$a\ddot{\tau}_h = \tau_m - \tau_h. \tag{31}$$

Then by applying the control law (25) with adaptation (26) we are in the case given in the Appendix, with the parameter c equal to 1. In this case the controlled system is asymptotically stable, i.e. it has infinite accuracy. This also shows that it is a good choice to adapt parameter c. When the environment changes dynamics from (6)–(7) to (31), the parameter changes its meaning and the controller achieves better accuracy.

Finally, we propose a similar adaptive algorithm that uses additional parameter $\hat{b}$ to estimate the human damping or dissipation. The proposed control law is

$$\tau_m = a(\ddot{\tau}_r - 2\lambda\dot{e} - \lambda^2 e) + \hat{b}\dot{\tau}_h + \hat{c}\tau_h - \delta \tag{32}$$

with adaptation dynamics given by

$$\dot{\hat{b}} = -\rho(s\dot{\tau}_h + \sigma\hat{b}), \quad \dot{\hat{c}} = -\rho(s\tau_h + \sigma\hat{c}). \tag{33}$$

This control law is expected to perform better because it can distinguish between the stiffness and the damping (dissipative) part of human dynamics. Stability of this controller can be analyzed in a similar way to the previous case but considering the linear human join model (7) which separates stiffness and damping forces. In this case, we can also prove the boundedness of human displacement $\tilde{q}$ and velocity $\dot{q}$.

THEOREM 3. *Given system (6)–(7), constrained to* $|h(\theta - q_0) + rd\dot{\theta}| \leq \Omega$, *and the adaptive control law (25)–(26), assuming a steady state reference model condition* $\tau_r(t) = \bar{\tau}_r$, *then state trajectories* $s(t)$, $\dot{q}$, $\tilde{q}$, $\tilde{c}(t)$, *and* $\tilde{b}(t)$ *are globally uniformly ultimately bounded.*

Theorem 3 uses the original findings of both Theorems 1 and 2. Control law (25)–(26) stabilizes the human displacement $\tilde{q}$ and discards the dynamics of q and $\dot{q}$.

5. Experimental Results

The experimental setup is the SEA prototype shown in Figure 3, comprising a DC torque motor connected in series to a spring and then to a metal bar simulating the support for a human limb. Two high precision encoders are used to measure motor position and spring displacement. Velocities are obtained by measuring pulse inter-periods, using hardware interrupts.

The control system runs on a standard PC equipped with a quadcore processor and a real-time Linux kernel. Real-time is obtained using a process with kernel-like priority and system sleep function with nanosecond granularity. The control process runs at 3 KHz and communicates with the motor drive and the sensor electronics via Ethercat protocol at the same rate.

System parameters have been estimated using a procedure similar to the one described in ref. [4] and reported in Table I. In the experiments, the metal support in Figure 3 has been replaced by a wood frame to create the worst-case working condition. This is because we use a direct drive

https://doi.org/10.1017/S0263574714001519 Published online by Cambridge University Press

Table I. System parameters.

Parameter	Symbol	Mean value
Spring Stiffness	k	1.040 Nm/rad
Torque constant	k_t	0.42 Nm/A
Motor inertia	J_m	0.00041 Kg/m^2
Wood load inertia	J_W	0.00025 Kg/m^2
Metal load inertia	J_M	0.00390 Kg/m^2
a	J_m/k	0.00039
c – wood load	$1 + J_m/J_W$	2.62
c – metal load	$1 + J_m/J_M$	1.10

Table II. Motor and human inertia pairs where $c \sim 2.5$.

Joint	Human inertia, J_h	Motor inertia, $n^2 J_m$	n
Hip (swing)	$\sim 0.5 \div 5$ Kg m^2	$\sim 0.8 \div 8$ Kg m^2	$\sim 200 \div 800$
Knee (swing)	~ 0.4 Kg m^2	~ 0.6 Kg m^2	$\sim 50 \div 250$
Elbow	~ 0.08 Kg m^2	~ 0.1 Kg m^2	$\sim 30 \div 100$
Wrist	~ 0.0015 Kg m^2	~ 0.002 Kg m^2	$\sim 15 \div 40$

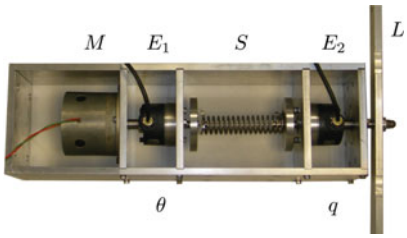

Fig. 3. (Colour online) The SEA prototype used as test bed. The motor M is connected to the torsional spring S and the angular quantities θ and q are measured by encoders E_1 and E_2 respectively. L is the arm support that is a pure inertial load when the system is not interacting with a human joint.

transmission and need to have a small load inertia (less or comparable with J_m) to get pessimistic values for parameter c, as defined in (8). With the wood load we achieve $c = 2.62$. To understand whether our setup is a representative of a real rehabilitation scenario, we report in Table II some pairs (human inertia, motor inertia) that are characterized by $c \sim 2.5$ (or equivalently $r \sim 1.5$), which defines sensitivity to environment dynamics. Approximate values for human inertia are derived from bio-mechanical measurements in refs. [8, 27]. We also report examples of transmission ratios n that are computed considering a motor shaft of $10^{-6} \div 10^{-5}$Kg m^2. Reported values are consistent to those seen in practical applications.

The objective of experiments is to test the controllers in the worst-case scenario when the system dramatically changes its dynamics. To this aim, we designed the following experiments. At the beginning we create a high impedance condition by holding the wood frame by hand and trying to be as stiff as possible ($c \sim 1$). Then after some seconds we release the frame to create a low-impedance condition ($c \sim 2.5$). The sequence can be repeated to test stability at impact when we hit the load to hold it for the second time. In this case we call the experiment "intermittent interaction test." Note that as the wood load inertia is very low, the impact velocity can be very high.

To have a baseline, we first show the behavior of PB controllers. The passive PID controller (3) is tuned with $P = 10$ and $D = 0.1$ and $I = 4$ with a 1 Hz roll-off frequency (accordingly to passivity constraints). The torque reference is low-pass filtered with a cut-off frequency of 35 Hz to avoid too oscillatory responses in case of discontinuities and to make a fair comparison with MRAC as we will use also a 35 -Hz reference model. Results of sinusoidal torque tracking are shown in Figure 4. Errors

https://doi.org/10.1017/S0263574714001519 Published online by Cambridge University Press

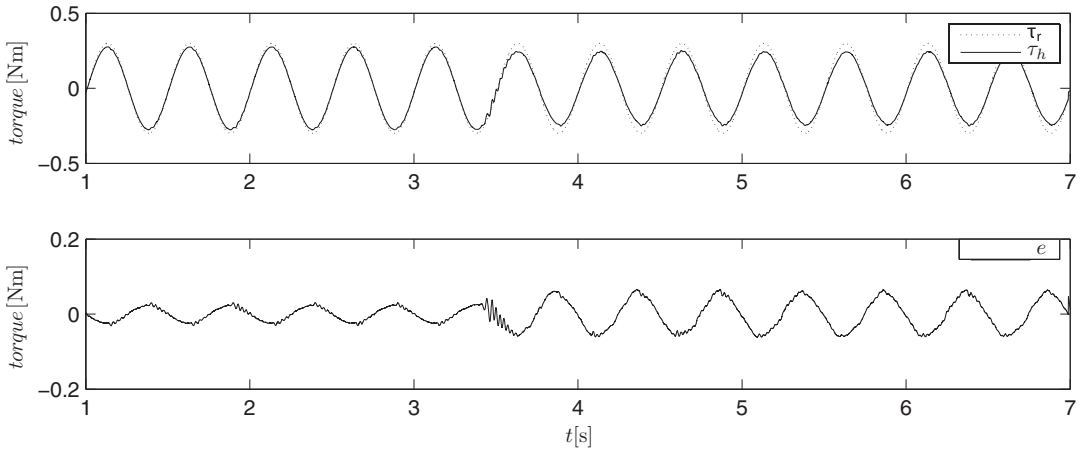

Fig. 4. Response of Algorithm (3) using a sinusoidal reference τ_r. First, the load is held by hand, and then released at about $t = 3.5$ s.

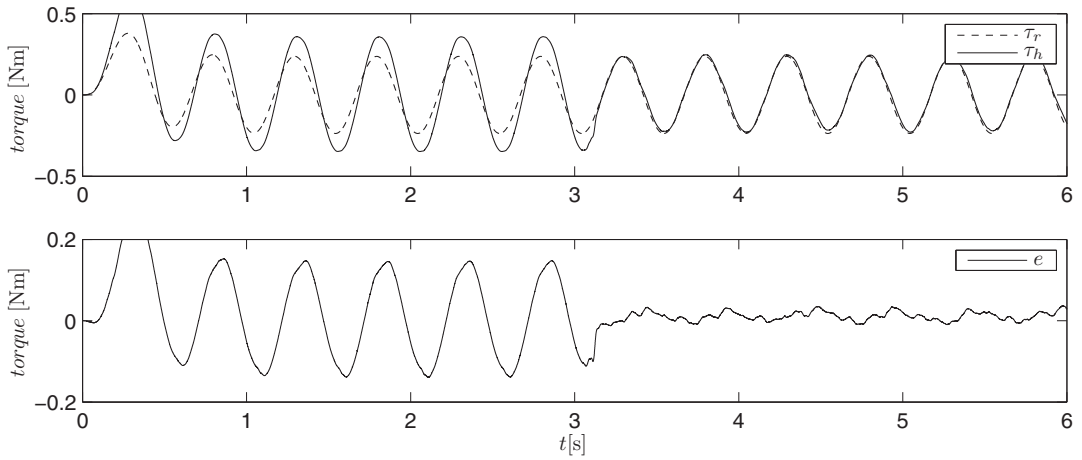

Fig. 5. Response of a PD controller tuned on free wood load condition. First, the load is held by hand, and then released at about $t = 3.0$ s.

are quite low in the case of high impedance, but when the load is released, errors increase and evident oscillations occur. To have high performance in the low-impedance condition, we avoid the integral term and use a fix-gain version of algorithm (25) considering $c = 2.62$. This algorithm is passive because by setting $\lambda = 120$ we have $P = a\lambda^2 - 2.62 > 0$ and $D = 2a\lambda > 0$. Figure 5 shows that while the response is accurate in the case of low impedance, we have significant overshoots when the impedance is high.

The outcomes of the proposed adaptive algorithms are shown in Figure 6–9. In all the following tests we used a critically damped 35-Hz reference model and a convergence rate, $\lambda = 120$. Larger values for λ lead to noise amplification. Estimated parameters are initialized to zero. The plotted error e is computed with respect to the reference model, thus it is not only a measure of accuracy but also of specification fulfillment. Figure 6 shows the behavior of algorithm (14) when only the high impedance is applied. It is possible to see a final very small error as well as convergence of parameters $\hat{b}$ and $\hat{c}$. Adaptation transient is kept slow in order to put in evidence the effects of parameter learning. In a real-life application, convergence can take less than one second without generating oscillations, as we will show in the following. We do not expect that parameters converge to their true value because estimation errors are proved to be marginally stable. In fact, in the experiment in Figure 6, parameters $\hat{d}$ $\hat{h}$ and $\hat{h}_o$ (not shown) remain low, especially in the case of $\hat{d}$ and $\hat{h}$ that remain very close to zero. Unfortunately, in the case of low impedance, when the load is unconstrained, this algorithm

https://doi.org/10.1017/S0263574714001519 Published online by Cambridge University Press

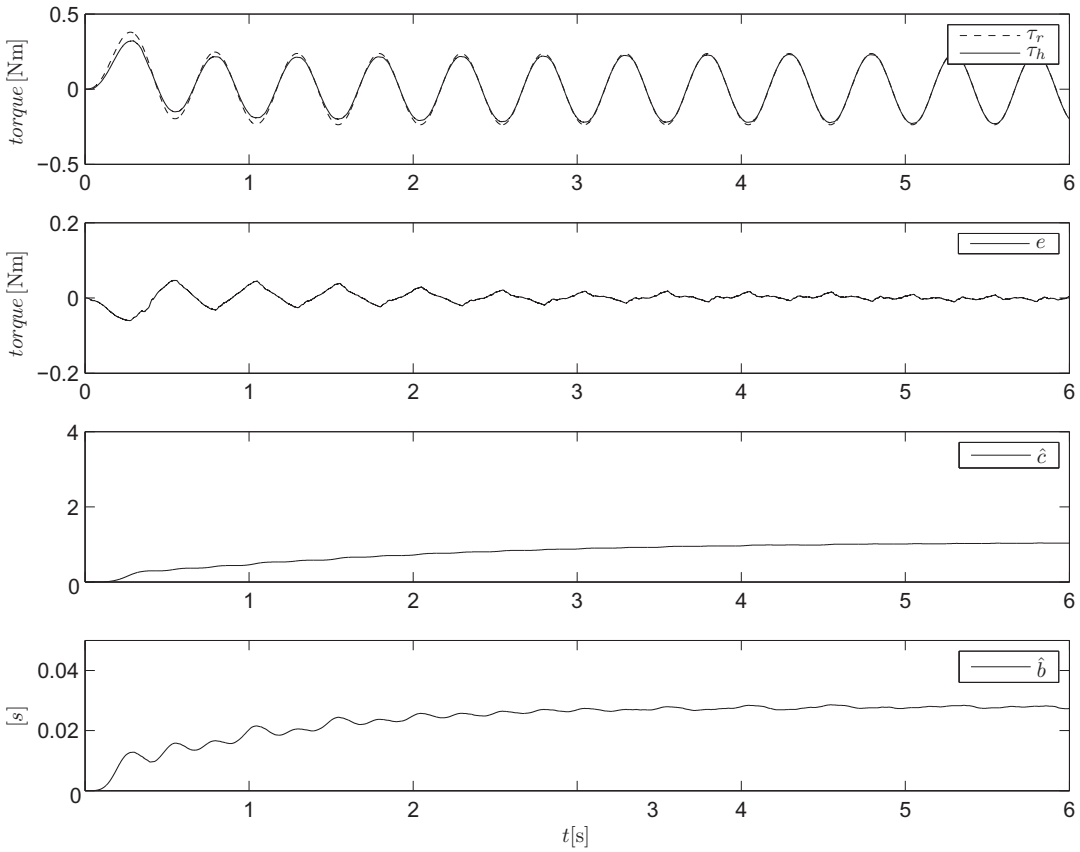

Fig. 6. Performance of control law (14) in response to a sinusoidal reference in the high impedance condition.

has worse behavior and we observed instability. This is probably due to the fact that in the case of low impedance, the load is let free and as a consequence the environment does not display any stiffness. This absence of stiffness information can cause a misbehavior of the estimation procedure which searches for a modeled stiffness actually missing in the real world. This causes both $\hat{h}$ and $\hat{h}_0$ estimates to be prone to divergence. Even from the point of view of system identification, when the environment does not display a stiffness/damping component, our model results over-parametrized, leading to the risk of a non-consistent estimation.

On the other hand, the simplified algorithm (25) shows a very stable behavior. We made a stress test by cyclically holding the load by hand and releasing it, thus testing also the impact stability. Figure 7 shows data from this "intermittent interaction test." Here, in particular, the load is first held by hand and released after about 5 s. Then, at time $t = 10$, the moving load is held again (a hit occurs) and then released after 5 s. Figure 7 shows that when the interaction changes, the parameter adapts showing noticeable decreasing error transients. Also, we have the evidence of a non-biased estimation. When the load is free, $\hat{c}$ converges to the correct value in Table I, otherwise when the load is held by hand, $c \sim 1$.

The controller (32) shows the best outcome, as shown in Figure 8 and 9. It combines the high tracking performance of algorithm (14) with the high robustness of its simplified version (25). In fact, when the joint is held by the human, it is subjected to some energy dissipation that leads the controller to change its derivative gain and achieve performance similar to that of Figure 6. In Fig. 7, this controller shows improved accuracy and similar robust behavior when the external impedance changes. These results are shown in Figure 8, where one can note the non-biased estimation of c.

In Figure 9, we show that the adaptation dynamics can be tuned to be very fast without degrading the maximum reachable precision nor the stability. If we compare this plot with the PB control responses reported in Figure 4 and 5, it is immediate to note improvements. A quantitative comparison of the described controllers is reported in Table III. Here each controller is tested in the high and low impedance condition separately. Root mean square (RMS) and maximum errors are reported for

https://doi.org/10.1017/S0263574714001519 Published online by Cambridge University Press

Table III. Comparison of RMS and maximum error (10^{-3}Nm).

	High impedance				Low impedance			
	Passive		Adaptive		Passive		Adaptive	
	PID	PD	$\hat{c}$	$\hat{b}, \hat{c}$	PID	PD	$\hat{c}$	$\hat{b}, \hat{c}$
RMS	27.3	102.6	9.3	**5.8**	69.0	15.1	13.9	**6.2**
σ_{RMS}	0.28	1.0	0.99	0.30	0.47	1.5	1.2	0.54
Max	41.4	146.5	17.2	**12.1**	99.6	26.3	18.9	**13.9**
σ_{Max}	0.67	1.1	2.6	1.1	0.84	2.9	3.6	1.3

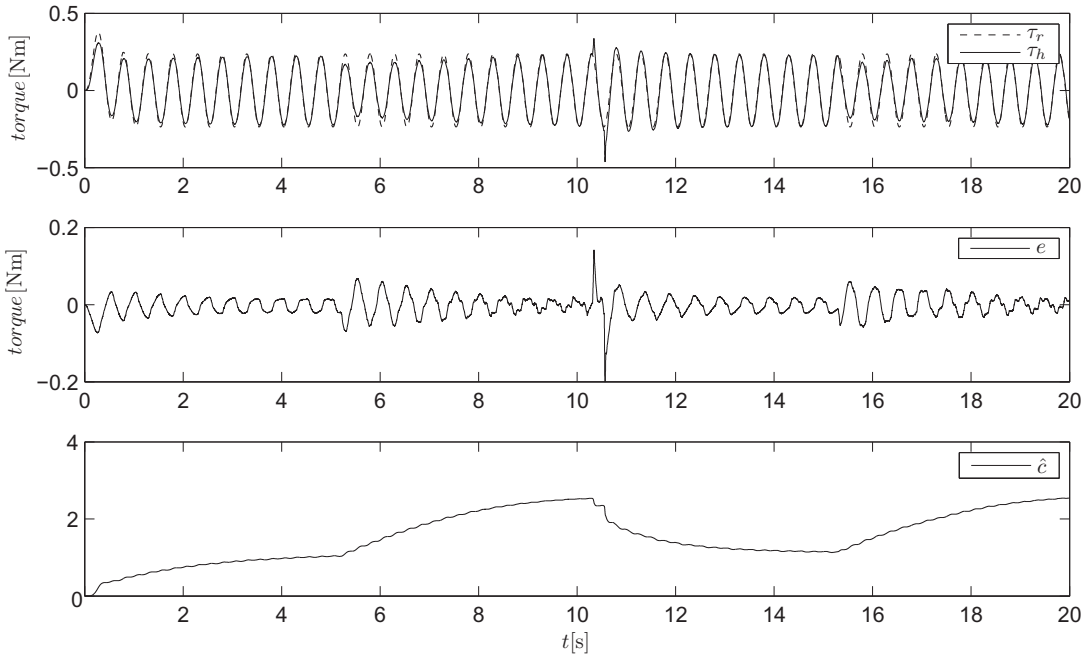

Fig. 7. The control law (25) in response to a sinusoidal reference in the "intermittent interaction test". The error peak occurs when we hit the load to hold it again.

each case. Because of the uncertain nature of pHRI, these indexes are computed for each reference period[2] and considered as random processes. Relative means and standard deviations are reported in Table III. Performance results greatly improved by the adaptive controller. Considering 3σ intervals, there are no statistically significant differences between performance in the high- and low-impedance conditions, especially in the case of control law (32), as represented graphically in Figure 7.

6. Conclusions

We proposed two simple and effective force control algorithms for SEAs (Eqs. (25) and (32)) that enable stable and predictable interaction with the human in both passive and active configurations. With respect to the existing PB controllers, the proposed solutions have several advantages. First, they can meet desired force control specifications even when the coupled dynamics changes; second, they do not need a tuning process as they are patient- and joint-specific self-tuning controllers; third, they proved to be very accurate. We think that these advantages are of paramount importance for control engineers to build rehabilitation or assistive devices. We demonstrated the quality of proposed controllers by discussing their theoretical properties and providing experimental validation. A brief

[2] We have a total of 240 periods for each controller, 120 in the high-impedance condition and 120 in the low-impedance condition.

https://doi.org/10.1017/S0263574714001519 Published online by Cambridge University Press

Table IV. Summary of paper results.

1. Control law 2. System model 3. Adaptation	Theoretical stability	Experimental outcome
1. Eq. (14) 2. Eqs. (6)–(7) 3. Param. b, c, d h, h_0	AS only when coupled with second-order linear impedance	High performance, poor stability (absence of environmental stiffness leads to instability).
1. Equation (25) 2. Equations (23)–(24) 3. Param. c	Globally UUB when coupled with the generic impedance (24)–(23). AS when coupled with "infinite" impedance (infinite inertia or stiffness or damping, etc.)	Medium performance, robust stability (it never goes to instability despite stress tests).
1. Equations (32) 2.Equations (6)–(7) 3. Param. b, c	Similar to the previous case. Here the boundedness proof also includes states $\tilde{q}$ and $\dot{q}$.	High performance, robust stability.

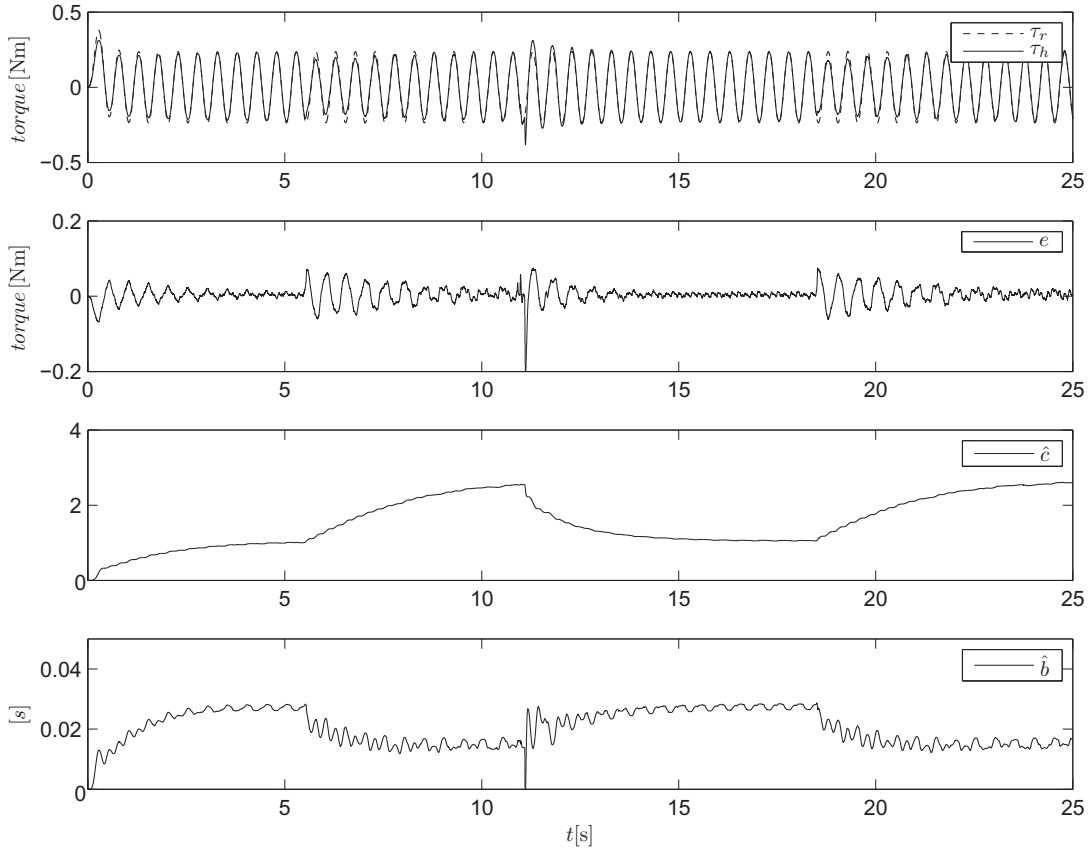

Fig. 8. The control law (32) in response to a sinusoidal reference in the "intermittent interaction test". The error peak occurs when we hit the load to hold it again.

view of achievement is summarized in Table IV, where for each controller we report related human joint model and adaptation parameters.

For the future work, we plan two objectives. The first is to investigate a passive version of the proposed adaptive approach. The second is to introduce adaptation mechanisms that are not only based on tracking errors but also on prediction errors.

https://doi.org/10.1017/S0263574714001519 Published online by Cambridge University Press

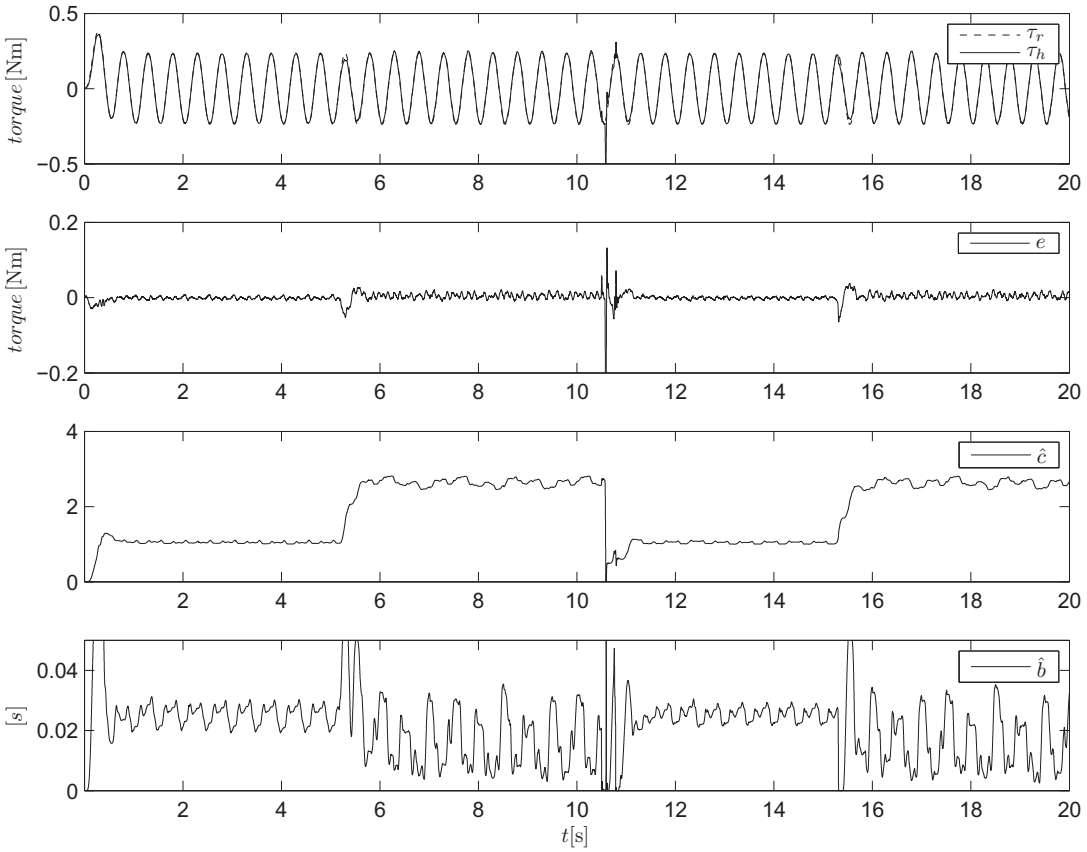

Fig. 9. The control law (32) with high adaptation gains in response to a sinusoidal reference in the "intermittent interaction test".

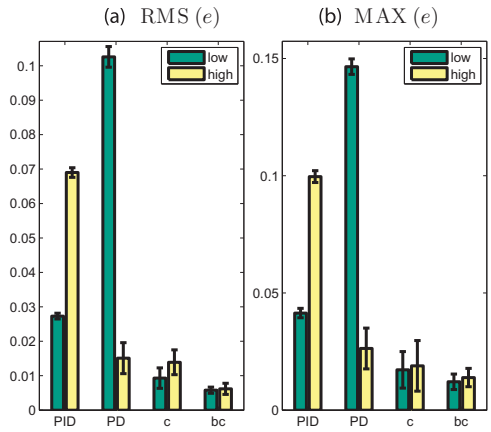

Fig. 10. (Colour online) RMS and maximum torque tracking error for passive PID, passive PD (tuned for low impedance), and adaptive controllers. Green and yellow bars represent data collected in high- and low-impedance conditions respectively. 3σ confidence intervals are shown.

References

1. S. P. Buerger and N. Hogan, "Complementary stability and loop shaping for improved human-robot interaction," *IEEE Trans. Robot.* **23**(2), 232–244 (2007).
2. S. Buerger and N. Hogan, "Relaxing Passivity for Human-Robot Interaction," *Proceedings of the 2006 IEEE/RSJ International Conference on Intelligent Robots and Systems* (Oct. 2006) pp. 4570–4575.
3. L. L. Cai, A. J. Fong, C. K. Otoshi, Y. Liang, J. W. Burdick, R. R. Roy and V. R. Edgerton, "Implications of assist-as-needed robotic step training after a complete spinal cord injury on intrinsic strategies of motor learning," *J. Neurosci.* **26**(41), 10564–10568 (Oct. 2006).

https://doi.org/10.1017/S0263574714001519 Published online by Cambridge University Press

4. A. Calanca, L. M. Capisani, A. Ferrara and L. Magnani, "MIMO closed loop identification of an industrial robot," *IEEE Trans. Control Syst. Technol.* **19**(5), 1214–1224 (2011).
5. A. Calanca, S. Piazza and P. Fiorini, "Force Control System for Pneumatic Actuators of an Active Gait Orthosis," *Proceedings of the 2010 3rd IEEE RAS and EMBS International Conference on Biomedical Robotics and Biomechatronics (BioRob),* Tokyo, Japan (Sep. 26–29, 2010) pp. 64–69.
6. A. Calanca, S. Piazza and P. Fiorini, "A motor learning oriented, compliant and mobile gait orthosis," *Appl. Bionics Biomech.* **9**(1), 15–27 (2012).
7. A. Duschau-Wicke, J. von Zitzewitz, A. Caprez, L. Lunenburger and R. Riener, "Path control: A method for patient-cooperative robot-aided gait rehabilitation," *IEEE Trans. Neural. Syst. Rehabil. Eng.* **18**(1), 38–48 (Feb. 2010).
8. W. S. Erdmann, "Geometry and inertia of the human body-review of research," *Acta Bioeng. Biomech.* **1**(1), 23–35 (1999).
9. M. Ferraro, J. J. Palazzolo, J. Krol, H. I. Krebs, N. Hogan and B. T. Volpe, "Robotaided sensorimotor arm training improves outcome in patients with chronic stroke," *Neurology* **61**(11), 1604–1607 (2003).
10. R. E. Kearney, R. B. Stein and L. Parameswaran, "Identification of intrinsic and reflex contributions to human ankle stiffness dynamics," *IEEE Trans. Biomed. Eng.* **44**(6), 493–504 (Jun. 1997).
11. K. Kong, S. Member and J. Bae, "Control of rotary series elastic actuator for ideal force-mode actuation in human-robot interaction applications," *IEEE/ASME Int. Conf. Mechatronics* **14**(1), 105–118 (2009).
12. H. I. Krebs, L. Dipietro, B. T. Volpe and N. Hogan, "Rehabilitation robotics: Performance-based progressive robot-assisted therapy," *Auton. Robots* **15**, 7–20 (2003).
13. K. Kyoungchul, M. Hyosang, J. Doyoung and T. Masayoshi, "Control of an exoskeleton for realization of aquatic therapy effects," *IEEE/ASME Trans. Mechatronics* **15**, 191–200 (2010).
14. K. S. Narendra and A. M. Annaswamy, "Robust Adaptive Control," **In:** *Proceedings of the 1984 American Control Conference* (ACC '84), Boston, MA (TFRT-1035) (Springer, New York, NY, 1985) 848 pp.
15. J. J. Palazzolo, "Robotic Technology to Aid and Assess Recovery and Learning in Stroke Patients," *Ph.D. Thesis* (Massachusetts Institute of Technology, 2005).
16. G. A. Pratt and M. M. Williamson, "Series Elastic Actuators," **In:** *IEEE International Conference on Intelligent Robots and Systems*, vol. 1 (1995) pp. 399–406.
17. G. A. Pratt, P. Willisson and C. Bolton, "Late Motor Processing in Low-Impedance Robots: Impedance Control of Series-Elastic Actuators," *American Control Conference* (2004) pp. 3245–3251.
18. J. Pratt, C.-M. Chew, A. Torres, P. Dilworth and G. Pratt, "Virtual model control: An intuitive approach for bipedal locomotion," *Int. J. Robot. Res.* **20**(2), 129–143 (2001).
19. J.-J. E. Slotine and W. Li, *Applied Nonlinear Control*, vol. 62 (Prentice Hall, Upper Saddle River, NJ, 1991).
20. R. B. Stein, E. P. Zehr, M. K. Lebiedowska, D. B. Popović, A. Scheiner and H. J. Chizeck, "Estimating mechanical parameters of leg segments in individuals with and without physical disabilities," *IEEE Trans. Rehabil. Eng.* **4**(3), 201–211 (Sep. 1996).
21. S. Stroeve, "Impedance characteristics of a neuromusculoskeletal model of the human arm I. Posture control," *Biol. Cybern.* **81**(5–6), 475–494 (Nov. 1999).
22. K. P. Tee, E. Burdet, C. M. Chew and T. E. Milner, "A model of force and impedance in human arm movements," *Biol. Cybern.* **90**(5), 368–375 (May 2004).
23. H. Vallery, "Stable and User-Controlled Assistance of Human Motor Function." *Ph.D. Thesis* (University of Munchen, Munich, Germany, 2009).
24. H. Vallery, R. Ekkelenkamp, H. van der Kooij and M. Buss, "Passive and Accurate Torque Control of Series Elastic Actuators," *Proceedings of the 2007 IEEE/RSJ International Conference on Intelligent Robots and Systems* (Oct. 2007) pp. 3534–3538.
25. H. Vallery, E. H. F. van Asseldonk, M. Buss and H. van der Kooij, "Reference trajectory generation for rehabilitation robots: Complementary limb motion estimation," *IEEE Trans. Neural Syst. Rehabil. Eng.* **17**(1), 23–30 (Feb. 2009).
26. Y. Xu and J. M. Hollerbach, "A robust ensemble data method for identification of human joint mechanical properties during movement," *IEEE Trans. Biomed. Eng.* **46**(4), 409–419 (Apr. 1999).
27. V. M. Zatsiorsky, *Kinetics of Human Motion* (Human Kinetics, Champaign, IL, 2002).

Appendix

A1 Stability analysis of control law (10) on model (5)

The following candidate Lyapuanov function for the controlled system, including the plant (5), the control law (10), and the adaptation law (12), is chosen,

$$V = \frac{1}{2}[as^2 + \frac{1}{\gamma}\tilde{c}^2] \geq 0,$$

https://doi.org/10.1017/S0263574714001519 Published online by Cambridge University Press

where $s = \dot{e} + \lambda e$ is a measure of the tracking error and $\tilde{c} = \hat{c} - c$ is the parameter estimation error. By computing the time derivative one can find

$$\dot{V} = as\dot{s} + \frac{1}{\gamma}\tilde{c}\dot{\tilde{c}}, \tag{A1}$$

where computation of $\dot{s}$ needs the knowledge of the closed loop dynamics. This can be obtained by substituting Eq. (10) into (5) leading to $\dot{s} = \frac{\tilde{c}\tau_h}{a} - \lambda s$ and then to

$$\dot{V} = -a\lambda s^2 + \tilde{c}s\tau_h + \frac{1}{\gamma}\tilde{c}\dot{\tilde{c}}. \tag{A2}$$

By applying the adaptation law $\dot{\tilde{c}} = \dot{\hat{c}} = -\gamma s\tau_h$ in (A2) we finally have $\dot{V} = -a\lambda s^2 \leq 0$ that implies global marginal stability for the system, thus bounded s and $\tilde{c}$. To prove convergence of s to zero, we can use Barbalat's lemma. Given a lower bounded V, it requires $\dot{V} \leq 0$ and $\dot{V}$ to be uniformly continuous in time, then it proves that $s \to 0$ for $t \to \infty$. A sufficient condition for uniform continuity is a bounded second-order derivative that can be computed as

$$\ddot{V} = -2\lambda\tilde{c}s\tau_h + 2a(\lambda s)^2. \tag{A3}$$

Then asymptotic stability of s can be proven, considering that we already proved the boundedness of s, e, and $\tilde{c}$ and the human force $\tau_h = \tau_r + e$ is limited if we apply the bounded desired force $r(t)$ to the stable reference model (9).

https://doi.org/10.1017/S0263574714001519 Published online by Cambridge University Press